Flow Curvature Effect on Darrieus Wind Turbine with Blade Pitching

Amalesh Chandra Mandal and Md. Quamrul Islam
Mechanical Engineering Department
Bangladesh University of Engineering & Technology, Dhaka

ABSTRACT

This paper presents a theoretical investigation of the predicted performance of a straight bladed Darrieus wind turbine with high chord radius ratio and blade pitching. For a high chord radius ratio turbine the flow on the turbine blade airfoil appears to be curvilinear in nature. An extension of the multiple streamtube theory is made by introducing the effect of the curved nature of flow occurring on the turbine blade.

INTRODUCTION

In order to predict the performance of a Darrieus wind turbine, the instantaneous local relative flow velocity and the local angle of attack are chosen as the values seen at infinity for an observer located at an arbitrary position on the blade. The velocity at infinity is assumed to be the vector sum of the free stream velocity and the tangential velocity at the blade supporting point. This assumption is valid only for a small chord radius ratio Darrieus turbine. For a high chord radius ratio turbine, the local angle of attack varies along the chord of turbine blade making the flow curvilinear in nature, as a result the angle of incidence is not constant along the chordwise direction. In the present analysis, a correction angle is introduced to take into account the curvilinear nature of flow. The local angle of attack obtained at the blade supporting point with the conventional method is modified by adding the correction angle. Lift drag characteristics are chosen corresponding to the modified angle of attack.

The calculated values incorporating the flow curvature effect are compared with those without flow curvature. Blade pitching is incorporated into the analysis. Due to the lack of experimental data with blade pitching the calculated results could not be correlated. However, it is expected that it would give a reasonable correlation.

The effect of the zero-lift-drag coefficient of a turbine is taken into account in the calculation [1]. Aspect ratio effect on the lift drag characteristics is also incorporated into the calculation [2]. Airfoil characteristics for NACA 0012 and NACA 0015 are considered in accordance with references [3],[4],[5] and [6].

DEVELOPMENT OF AERODYNAMIC THEORY

For a high chord radius ratio Darrieus turbine, the direction of relative flow velocity is varied along the chord as shown in Fig. 1, which results in the variation of local angle of attack along the chord and the flow becoming curvilinear in nature.

Flow curvature effect, which is presented in reference [1], is added with the multiple streamtube model [7] including real lift drag characteristics, and the effect of blade pitching is incorporated into

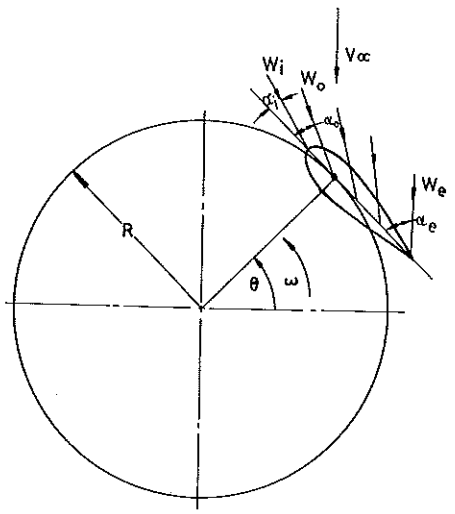

Fig. 1. Typical variation of relative flow velocity direction for a high chord radius ratio Darrieus turbine.

the model.

Since for the multiple streamtube model the induced velocity $V_a = V_{au} = V_{ad}$, it follows that the relative flow velocity for no flow curvature effect $W_o = W_{ou} = W_{od}$ and the angle $\beta_o = \beta_{ou} = \beta_{od}$. W_o and β_o may be expressed as,

$$\frac{W_o}{V_a} = \left[\left(\frac{R\omega}{V_\infty} / \frac{V_a}{V_\infty}\right) + \cos\theta\right]^2 + \sin^2\theta \tag{1}$$

$$\beta_o = \tan^{-1}\left[\frac{\sin\theta}{\left(\frac{R\omega}{V_\infty} / \frac{V_a}{V_\infty}\right) + \cos\theta}\right] \tag{2}$$

Lift coefficient C_l is obtained from [1],

$$C_l = 2\pi k \sin\alpha \tag{3}$$

Corresponding to the angle of attack α, the lift coefficient C_l is taken from the airfoil data and the parameter k is calculated. The parameter k is included to consider the real lift characteristics. For an inviscid and incompressible fluid, the equivalent force on the blade airfoil in the upstream side may be written in the form (Fig. 2),

$$\vec{F}_{u_{eq}} = \rho H \vec{W}_{u_{eq}} \times \vec{\Gamma}_{u_{eq}} \tag{4}$$

Where the equivalent relative flow velocity in the upstream side is,

$$\vec{W}_{u_{eq}} = \vec{W}_{ou} + \Delta\vec{W}_u \tag{5}$$

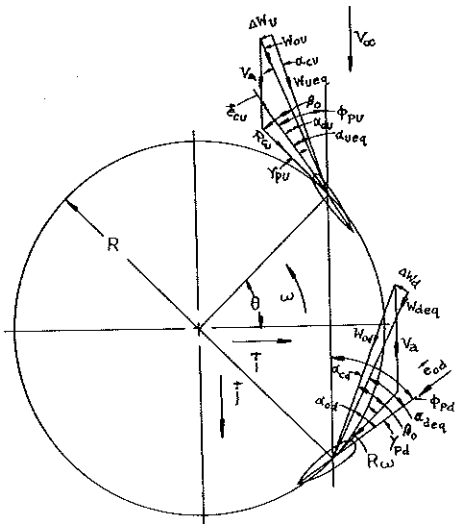

Fig. 2. Velocity diagram on the blade airfoil with pitching in an equivalent flow condition due to flow curvature.

ΔW_u is the velocity which makes a relationship between $W_{u_{eq}}$ and W_{ou}, being one of the members in the vector triangle for the upstream side (Fig. 2). Introducing the value of $\vec{W}_{u_{eq}}$ in the Eq. (4), one may obtain,

$$\vec{F}_{u_{eq}} = \rho H \vec{W}_{ou} \times \vec{\Gamma}_{u_{eq}} + \rho H \Delta \vec{W}_u \times \vec{\Gamma}_{u_{eq}} \tag{6}$$

Since in the analysis it is assumed that $W_{u_{eq}} \approx W_{ou}$ (ref. [1]) and the incidence correction angle α_{cu} is very small, as a result ΔW_u is negligible in comparison to W_{ou}. So, in the above Eq. (6), the second term containing ΔW_u can be assumed to be negligible in comparison to the first term containing W_{ou}, hence one finds,

$$\vec{F}_{u_{eq}} = \rho H \vec{W}_{ou} \times \vec{\Gamma}_{u_{eq}} \tag{7}$$

Similarly, the equivalent force on the downstream blade airfoil is found as,

$$\vec{F}_{d_{eq}} = \rho H \vec{W}_{od} \times \vec{\Gamma}_{d_{eq}} \tag{8}$$

Referring to Fig. 2, the relative flow velocities in the upstream and downstream sides are found as,

$$\vec{W}_{ou} = R\omega \sin\theta \, \vec{i} + (V_a + R\omega \cos\theta) \, \vec{j} \tag{9}$$

$$\vec{W}_{od} = -R\omega \sin\theta \, \vec{i} + (V_a + R\omega \cos\theta) \, \vec{j} \tag{10}$$

The circulation due to flow curvature effect on the upstream blade airfoil can be expressed as,

$$\vec{\Gamma}_{u_{eq}} = \pi k_{u_{eq}} C \vec{W}_{u_{eq}} \times \vec{e}_{cu} \tag{11}$$

Now, introducing the value of $\vec{W}_{u_{eq}}$ from the Eq. (5) and neglecting the term associated with ΔW_u,

$$\vec{\Gamma}_{u_{eq}} = \pi k_{u_{eq}} C \vec{W}_{ou} \times \vec{e}_{cu} \tag{12}$$

Similarly, the equivalent circulation on the downstream blade airfoil can be expressed as,

$$\vec{\Gamma}_{d_{eq}} = \pi k_{d_{eq}} C \vec{W}_{od} \times \vec{e}_{cd} \tag{13}$$

The unit vectors $\vec{e}_{cu}$ and $\vec{e}_{cd}$ may be expressed as (referring to Fig. 2),

$$\vec{e}_{cu} = \sin \phi_{pu} \vec{i} + \cos \phi_{pu} \vec{j} \tag{14}$$

$$\vec{e}_{cd} = -\sin \phi_{pd} \vec{i} + \cos \phi_{pd} \vec{j} \tag{15}$$

Now, the expressions of the equivalent force on the upstream blade airfoil are found from the Eqs. (7), (9), (12) and (14) while the expressions of the equivalent force on the downstream blade airfoil are obtained from the Eqs. (8), (10), (13) and (15). The terms associated with the unit vector $\vec{j}$ in each of the expressions of equivalent forces for upstream and downstream sides are the streamwise forces. Adding streamwise forces on the upstream and downstream blade airfoils and replacing C by NC $\delta\theta/2\pi$ for an assumption of an infinite number of blades distribution, the expression of the net equivalent streamwise elemental force becomes,

$$\begin{aligned}\delta F_{D_{eq}} = {}& \tfrac{1}{2} \rho N C H R \omega \sin\theta \,[k_{u_{eq}}(V_a \sin\phi_{pu} - R\omega \sin\gamma_{pu}) \\ & + k_{d_{eq}}(V_a \sin\phi_{pd} + R\omega \sin\gamma_{pd})]\,\delta\theta\end{aligned} \tag{16}$$

The elemental force along the streamwise direction due to the rate of change of momentum may be obtained in the form,

$$\delta F_D = 2\rho R H V_a \sin\theta (V_\infty - V_a)\delta\theta \tag{17}$$

Now, balancing the net equivalent elemental streamwise forces from the Eq. (16) with the elemental streamwise force due to the rate of change of momentum from the Eq. (17), one may obtain the expression of the induced velocity as,

$$\frac{V_a}{V_\infty} = 1 - \tfrac{1}{4} \cdot \frac{NC}{R} \cdot \frac{R\omega}{V_\infty} \left[k_{u_{eq}} \left(\sin\phi_{pu} - \frac{R\omega/V_\infty}{V_a/V_\infty} \sin\gamma_{pu}\right) + k_{d_{eq}} \left(\sin\phi_{pd} + \frac{R\omega/V_\infty}{V_a/V_\infty} \sin\gamma_{pd}\right)\right] \tag{18}$$

The equivalent factors $k_{u_{eq}}$ and $k_{d_{eq}}$ may be found from,

$$k_{u_{eq}} = \frac{C_{lu_{eq}}}{2\pi \sin\alpha_{u_{eq}}} \tag{19}$$

$$k_{d_{eq}} = \frac{C_{ld_{eq}}}{2\pi \sin\alpha_{d_{eq}}} \tag{20}$$

where $\alpha_{u_{eq}}$ and $\alpha_{d_{eq}}$ are obtained from, in accordance with reference[1],

$$\alpha_{u_{eq}} = \alpha_{ou} + \alpha_{cu} \tag{21}$$

$$\alpha_{d_{eq}} = \alpha_{od} - \alpha_{cd} \tag{22}$$

Incidence correction angle α_c is obtained from reference [1],

$$\alpha_c = \tan^{-1}\left[\frac{1-\cos(\beta/2)}{\sin(\beta/2)}\right] \tag{23}$$

where

$$\beta = (\alpha_e - \alpha_i) \tag{24}$$

α_{ou} and α_{od} may be found from

$$\alpha_{ou} = (\beta_o - \gamma_{pu}) \tag{25}$$

$$\alpha_{od} = (\beta_o + \gamma_{pd}) \tag{26}$$

The equivalent torque including flow curvature effect for blade length of H,

$$Q_{eq} = (F_{t_{u_{eq}}} + F_{t\,d_{eq}})R + (M_{u_{eq}} + M_{d_{eq}}) \tag{27}$$

The overall equivalent torque coefficient including flow curvature is defined as,

$$C_{Q_{eq}} = \frac{Q_{eq}}{\frac{1}{2}\rho\, A\, V_\infty^2\, R} \tag{28}$$

Equivalent tangential forces and equivalent blade pitching moments may be expressed as,

$$F_{tu_{eq}} = \tfrac{1}{2} C_{tu_{eq}} \rho W_{u_{eq}}^2 CH \tag{29}$$

$$F_{td_{eq}} = \tfrac{1}{2} C_{td_{eq}} \rho W_{d_{eq}}^2 CH \tag{30}$$

$$M_{u_{eq}} = \tfrac{1}{2} C_{mu_{eq}} \rho W_{u_{eq}}^2 C^2 H \tag{31}$$

$$M_{d_{eq}} = \tfrac{1}{2} C_{md_{eq}} \rho W_{d_{eq}}^2 C^2 H \tag{32}$$

From the Eqs. (27) to (32), one may obtain the expression of $C_{Q_{eq}}$ as,

$$C_{Q_{eq}} = \frac{1}{4\pi}\frac{NC}{R}\int_0^\pi \frac{W_o^2}{V_\infty^2}\left[(C_{tu_{eq}} + C_{td_{eq}}) + \frac{C}{R}(C_{mu_{eq}} + C_{md_{eq}})\right] d\theta \tag{33}$$

The values of $C_{tu_{eq}}$ and $C_{td_{eq}}$ may be respectively found from,

$$C_{tu_{eq}} = C_{lu_{eq}} \sin \beta_{u_{eq}} - C_{du_{eq}} \cos \beta_{u_{eq}} \tag{34}$$

$$C_{td_{eq}} = C_{ld_{eq}} \sin \beta_{d_{eq}} - C_{dd_{eq}} \cos \beta_{d_{eq}} \tag{35}$$

where

$$\beta_{u_{eq}} = \beta_o + \alpha_{cu} \tag{36}$$

and

$$\beta_{d_{eq}} = \beta_o - \alpha_{cd} \tag{37}$$

The equivalent turbine power coefficient is obtained from,

$$C_{p_{eq}} = C_{Q_{eq}} \lambda \tag{38}$$

Equation (33) may be applied for no blade pitching by inserting $\gamma_p = o$. The same equation may also be used for no flow curvature effect by considering the incidence correction angle equal to zero. These will be followed to obtain comparative results.

Effect of zero-lift-drag coefficient is introduced in the calculation. It has a strong influence on performance characteristics. It depends on chord-radius-ratio as mentioned in the reference [8]. Zero-lift-drag coefficient corrected for chord-radius ratio is expressed according to reference [1] as,

$$C_{do_c} = C_{do} + b\,[C/R - (C/R)_o] \tag{39}$$

where (C/R) is any chord radius ratio, $(C/R)_o$ indicates (C/R) value up to which correction of C_{do} value due to chord radius ratio is not necessary, b is constant, C_{do} may be obtained from reference [9],

$$C_{do} = C_{do_r}(R_e/R_{er})^n \tag{40}$$

Value of exponent n may be obtained from reference [1]. Comparison of recent two dimensional experimental results of C_{do} from Eppler [10], Reuter, Jr. [11] and Willmer [5] with the calculated values of C_{do} in Fig. 3, proves the validity of the expression of zero-lift-drag coefficient.

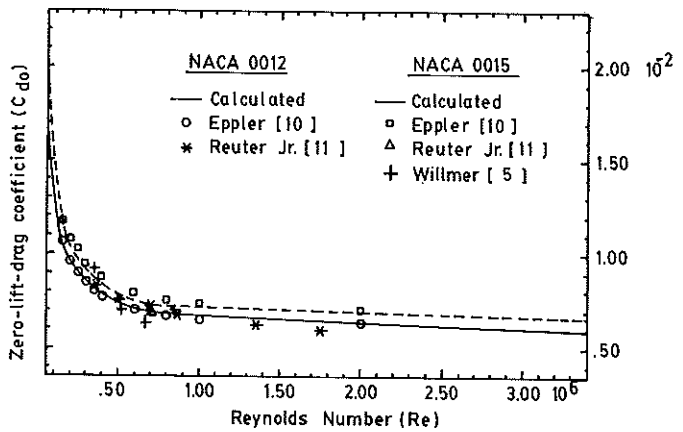

Fig. 3. Comparisons of experimental and analytical zero-lift-drag coefficients for the airfoils NACA 0012 and NACA 0015.

RESULTS AND DISCUSSIONS

Figure 4 shows the comparisons of the calculated values by simple multiple streamtube theory, multiple streamtube theory with curvature effect (present), multiple streamtube theory with Migliore's flow curvature model, multiple streamtube theory with Muraca's curvature model and the experimental data. These experimental data are presented by Migliore et al. [8] for the outdoor test model of West Virginia University. Blade pitching is not incorporated into this turbine. Experimental data have not been available with blade pitching up until now. It is observed from this figure that the correlation is reasonable with the calculated values by multiple streamtube model including flow curvature effect and it occurs at the higher tip speed ratio side only. Appreciable differences are observed between the values calculated using Migliore's model and the experimental data. The calculated values compared to those obtained by using Migliore's method even give deteriorating power compared to those obtained by using the simple multiple streamtube model. Applying

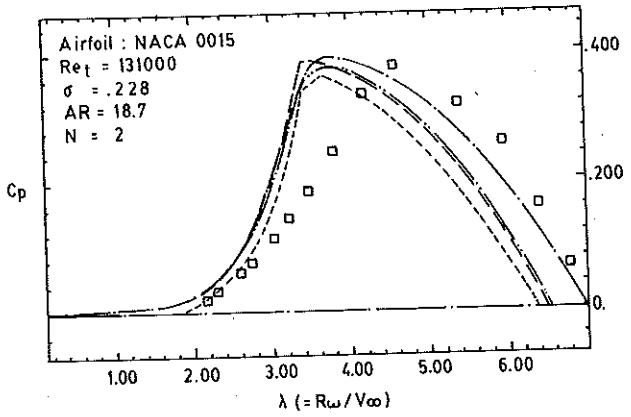

Fig. 4. Comparisons of experimental and calculated overall power coefficients.
—— calc. (simple multiple streamtube)
—·— calc. (multiple streamtube with flow curvature, present)
□ expt. (3m - WVU[13])
----- calc. (multiple streamtube with curvature, Migliore[8])
—··— calc. (multiple streamtube with curvature, Muraca[12])

Migliore's model, the power increases in the upstream side and decreases in the downstream side and the net effect reduces the total power. Using the present flow curvature model, power increases in the upstream side and decreases in the downstream side and the net power becomes positive. Muraca's model shows very negligible variations in the power coefficients in comparison to those with the simple multiple streamtube model. Using Muraca's model, the power rises in the upstream side and decreases in the downstream side but the net effect becomes nearly zero thereby making negligible variations in the power coefficient values. In the lower tip speed ratio side the correlation is bad. According to Cardona [14], this discrepancy is due to dynamic stall effect and he has therefore proposed a modified dynamic stall model to overcome this.

Comparisons of the calculated values of overall power and torque coefficients obtained by using simple multiple streamtube model and multiple streamtube model with flow curvature effect at various fixed pitchings (positive) are shown in Figs. 5 and 6 respectively. In the analysis, pitching is said to

be positive for the blade nose rotating in the outward direction from the blade flight path. The results in these figures are shown employing pitching of blade for the West Virginia University outdoor test model [13]. It is observed from these figures that by including flow curvature effect in the calculation, the performance characteristics are in general higher. It is also observed from these figures that with the application of fixed pitching, the rotor power always decreases. The higher is the pitching, the lower is the power coefficient, as Fig. 5 reveals.

In corporating fixed blade pitching, the angle of attack decreases in the upstream side and increases in the downstream side. So the blade airfoil lift coefficient drops in the upstream side and

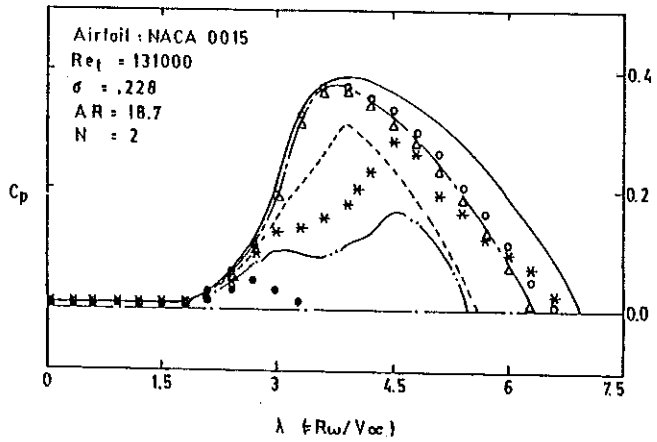

Fig. 5. Variations of overall power coefficients with tip speed ratios at different fixed blade pitchings.

Calculated:	Simple multiple streamtube theory				Multiple streamtube with curvature			
Symbol:	O	Δ	*	o	——	—·—	-----	—··—
Pitch (deg.):	0	2	5	7	0	2	5	7

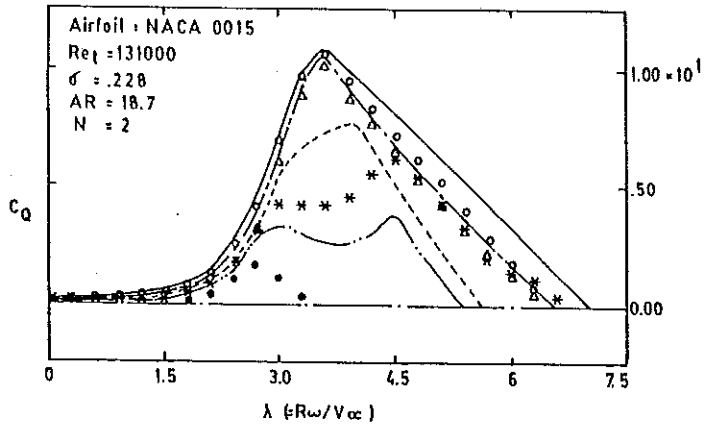

Fig. 6. Variations of overall torque coefficients with tip speed ratios at different fixed blade pitchings.

Calculated:	Simple multiple streamtube theory				Multiple streamtube with curvature			
Symbol:	O	Δ	*	o	——	—·—	-----	—··—
Pitch (deg.):	0	2	5	7	0	2	5	7

rises in the downstream side which is the outcome of the lower tangential force coefficients in the upstream side and higher tangential force coefficients in the downstream side in general. But, the increased angles of attack in the downstream side sometimes go beyond stalling angle in a few stations which again are the causes of reduced tangential force coefficients. However, the net effect always reduces the power coefficients.

Figures 7 and 8 present the comparisons of the induced velocities and local angles of attack by using the simple multiple streamtube model and the multiple streamtube model with flow curvature effect. The results are obtained for the West Virginia University test model [13] incorporating fixed blade pitching of 5 degrees and at a constant tip speed ratio of 4.5. One may observe from Fig. 7 that there appear remarkable differences of induced velocities in some range of azimuth angles while it may be seen from Fig. 8 that there occur appreciable variations of local angles of attack calculated by using

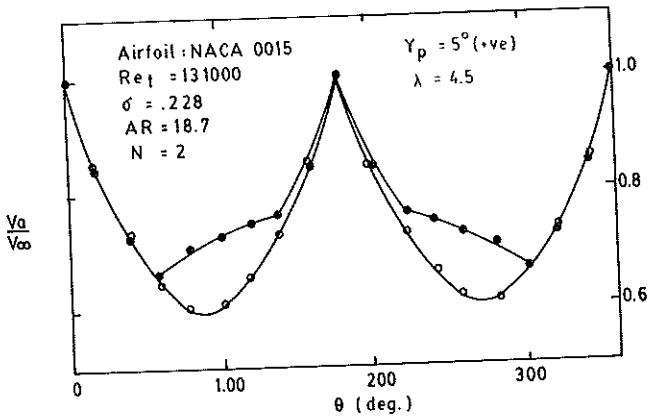

Fig. 7. Comparisons of induced velocity ratios.
● Calc. (simple multiple streamtube theory)
O Calc. (multiple streamtube theory with curvature effect)

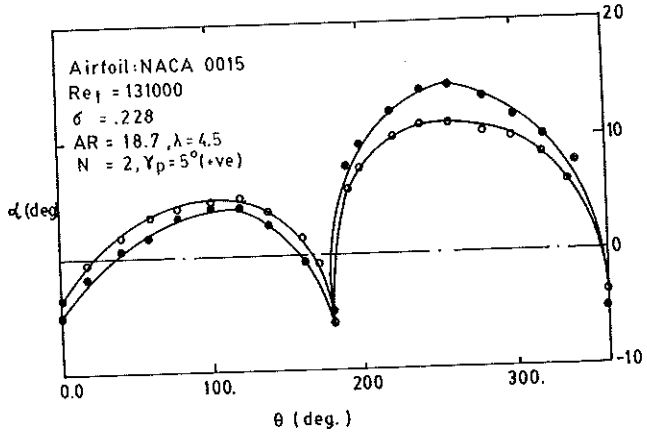

Fig. 8. Comparisons of local angles of attack.
● Calc. (simple multiple streamtube theory)
O Calc. (multiple streamtube theory with curvature effect)

a simple multiple streamtube model and a multiple streamtube model with curvature effect. According to the present multiple streamtube model including flow curvature effect, local angle of attack increases in the upstream side and decreases in the downstream side. This can be seen clearly from Fig. 8 showing local angles of attack distribution with azimuth angle by two models.

In Figs. 9 and 10, local, non-dimensional tangential and normal forces at fixed blade pitching of 5 degrees and at constant tip speed ratio of 4.5 calculated by using a simple multiple streamtube model are compared with those calculated by using a multiple streamtube model including flow curvature effect. Incorporating flow curvature effect into the multiple streamtube model, the local angle of attack increases in the upstream side and decreases in the downstream side which is the outcome of higher tangential forces in the upstream side and lower tangential forces in the downstream side. However,

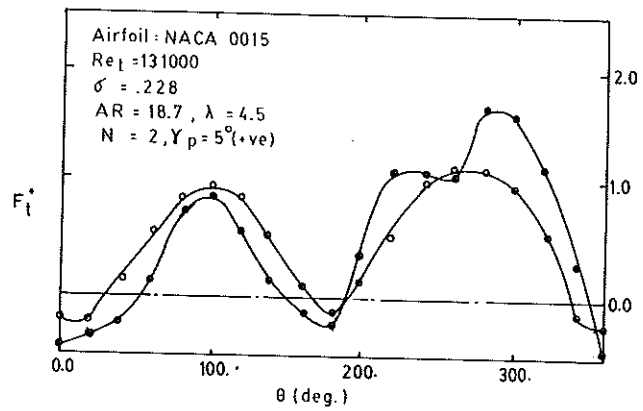

Fig. 9. Comparisons of local non-dimensional tangential forces with azimuth.
● Calc. (simple multiple streamtube theory)
O Calc. (multiple streamtube theory with curvature effect)

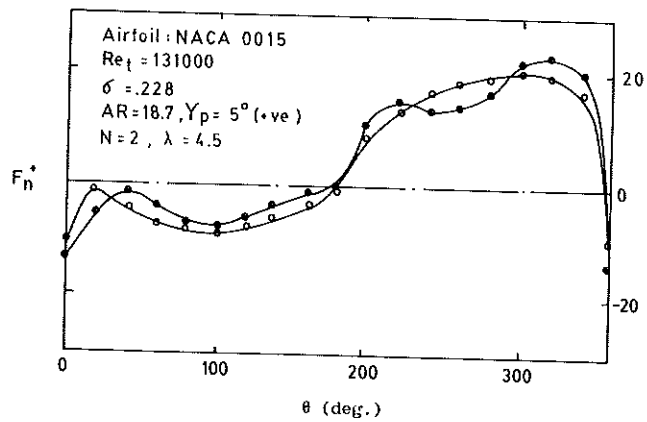

Fig. 10. Comparisons of local non-dimensional normal forces with azimuth.
● Calc. (simple multiple streamtube theory)
O Calc. (multiple streamtube theory with curvature effect)

with regard to the increasing local angle of attack value: if stalling appears the lift coefficient drops, resulting in lower tangential forces which may be observed from Fig. 9 around an azimuth angle of 250 degrees.

In the higher tip speed ratio range the calculated induced velocity ratios go below the theoretical limit of 0.5 for a few stations. For the station where there is such a problem, convergence is started with the first assumed value of induced velocity ratio 0.5 and the first iterated value is chosen as the required induced velocity ratio. Since this sort of problem appears only in few stations it is assumed that it has negligible influence on the calculated values.

CONCLUSIONS

In order to predict the performance of a vertical-axis Darrieus wind turbine, consideration of the flow curvature effect is very important for a large chord-radius ratio Darrieus wind turbine.

Consideration of flow curvature effect gives improved performance prediction even for a wind turbine having small chord-radius ratio.

To obtain the local forces on the turbine blade, calculation, including flow curvature effect, is necessary for a high as well as low chord-radius ratio Darrieus turbine.

Using the values of zero-lift-drag coefficient from the given analytical expressions and applying the present model of flow curvature with Wilson's multiple streamtube theory using real lift drag characteristics, it is possible to predict the performance with reasonable accuracy for a large chord-radius ratio Darrieus turbine.

The advantage of using the present method of flow curvature effect is that lift-drag characteristics of a symmetrical airfoil can be applied.

NOMENCLATURE

A	projected frontal area of turbine
AR	aspect ratio = H/C
C	blade chord
C_d	blade drag coefficient
C_{do}	zero-lift-drag coefficient
C_{do_c}	C_{do} value corrected for chord radius ratio
C_{do_r}	reference zero-lift drag coefficient
C_l	blade lift coefficient
C_m	blade pitching moment coefficient
C_n	normal force coefficient
C_P	turbine overall power coefficient
C_Q	turbine overall torque coefficient
C_t	tangential force coefficient
$\vec{e}_c$	unit vector along chordal direction

F	force on blade airfoil
F_D	turbine drag in streamwise direction
F_n^+	non-dimensional normal force = $C_n (W/V_\infty)^2$
F_t	tangential force
F_t^+	non-dimensional tangential force = $C_t (W/V_\infty)^2$
H	height of turbine
$\vec{i}, \vec{j}$	unit vectors, one normal to the other
k	factor to include real lift value
M	blade pitching moment
N	number of blades
Q	overall torque
R	turbine radius
R_e	local Reynolds number = WC/υ
R_{er}	reference Reynolds number corresponding to C_{do_r}
R_{et}	turbine speed Reynolds number = RWC/υ
R_{ew}	wind speed Reynolds number = $V_\infty C/\upsilon$
V_a	induced velocity
V_∞	wind velocity
W	relative flow velocity
W_o	relative flow velocity appearing in rectilinear flow
α	angle of attack
α_c	incidence correction angle due to flow curvature
α_o	angle of attack appearing in rectilinear flow
β	$(\alpha_c - \alpha_i)$
β_o	angle between relative flow velocity (W_o) direction and tangent to blade flight path at blade fixing point
γ_p	blade pitch angle
Γ	circulation per unit length
θ	azimuth angle
λ	tip speed ratio = $\frac{R\omega}{V_\infty}$
υ	kinematic viscosity
ρ	fluid density
σ	solidity = NC/R
ϕ_p	angle between chordal and free stream velocity directions
ω	angular velocity

Subscripts

d	downstream side
e	trailing edge point
eq	equivalent conditions due to flow curvature
i	leading edge point
u	upstream side

REFERENCES :

1. Hirsch, Ch. and A. C. Mandal (1984), Flow curvature effect on vertical axis Darrieus wind turbine having high chord radius ratio, *Proceedings of the First European Wind Energy Conference,* Hamburg, Oct. 22-26, 1984, pp.G.7 - 405 - 410
2. Clancy, L. C. (1978), *Aerodynamics,* A Pitman International Text, 2nd Edition.
3. Sheldahl, R. E. and B. F. Blackwell (1976), Aerodynamic characteristics of four symmetrical airfoil sections through 180° angle of attack at low Reynolds Number, *Vertical Axis Wind Turbine Technology Workshop,* May 17-20, 1976.
4. Jacob E. N. and A. Sherman (1937), *Airfoil Section Characteristics as Affected by Variations of the Reynolds Number,* NACA-TR-586, Sept. 1937.
5. Willmer, A.C. (1979), Low Reynolds Number Tests on the NACA 0015 Section, *1st BWEA Workshop,* April 1979, pp. 109-116.
6. Sharpe, D.J. (1977), *A Theoretical and Experimental Study of the Darrieus Vertical Axis wind Turbines,* Kingston Polytechnic, Oct. 1977.
7. Wilson, R.E. and P.B.S. Lissaman (1974), *Applied Aerodynamics of Wind Power Machines,* Oregon State University, May 1974.
8. Migliore, P.G., W.P. Wolfe and J.B. Fannuci (1980), Flow curvature effects on Darrieus turbine blade aerodynamics, *Journal of Energy,* Vol. 4. No. 2, March-April, pp. 49-55.
9. Declere, W., D.V. Aerschot and C.H. Hirsch (1981), The effects of Reynolds Number on the performance characteristics of Darrieus windmills with Troposkien and straight-blades, *Proceedings of the International Colloquium on Wind Energy,* Brighton, August 1981, pp. 243-248.
10. Eppler, R. (1978), Turbulent airfoil for general aviation , *Journal of Aircraft,* Vol. 15, Feb., pp. 93-99.
11. Reuter, R.C. Jr. and R.E. Sheldahl (1976), *Sandia Vertical Axis Wind Turbine Project,* Sandia Laboratories Report, SAND 76-0581.
12. Muraca, R.J., M.V. Stephens and J.R. Dagenhart (1975), *Theoretical Performance of Cross-Wind Axis Turbines with Results for a Catenary Vertical Axis Configuration,* NASA TMX-72662.
13. Migliore, P.G. and W.P. Wolfe (1980), *The Effects of Flow Curvature on the Aerodynamics of Darrieus Wind Turbines,* Dept. of Aerospace Engineering, WVU, Morgantown.
14. Cardona, J.L. (1984), Flow curvature and dynamic stall simulated with an aerodynamic free-vortex model for VAWT, *Wind Engineering,* Vol. 8, No. 3, pp. 135-143.
15. Mandal, A.C. (1986), *Aerodynamics and Design Analysis of Vertical Axis Darrieus Wind Turbines,* Ph.D. Thesis, Vrije Universiteit Brussel.